Purinergic Signalling (2006) 2:545–557
DOI 10.1007/s11302-006-9004-4

ORIGINAL ARTICLE

Excitatory effect of ATP on rat area postrema neurons

Masaru Sorimachia · Minoru Wakamoria · Norio Akaikeb

Received: 11 October 2005 / Accepted: 26 January 2006 / Published online: 30 May 2006

Abstract ATP-induced inward currents and increases in the cytosolic Ca^{2+} concentration ($[Ca]_{in}$) were investigated in neurons acutely dissociated from rat area postrema using whole-cell patch-clamp recordings and fura-2 microfluorometry, respectively. The ATP-induced current (I_{ATP}) and $[Ca]_{in}$ increases were mimicked by 2-methylthio-ATP and ATP-γS, and were inhibited by P2X receptor (P2XR) antagonists. The current–voltage relationship of the I_{ATP} exhibited a strong inward rectification, and the amplitude of the I_{ATP} was concentration-dependent. The I_{ATP} was markedly reduced in the absence of external Na^+, and the addition of Ca^{2+} to Na^+-free saline increased the I_{ATP}. ATP did not increase $[Ca]_{in}$ in the absence of external Ca^{2+}, and Ca^{2+} channel antagonists partially inhibited the ATP-induced $[Ca]_{in}$ increase, indicating that ATP increases $[Ca]_{in}$ by Ca^{2+} influx through both P2XR channels and voltage-dependent Ca^{2+} channels. There was a negative interaction between P2XR- and nicotinic ACh receptor (nAChR)-channels, which depended on the amplitude and direction of current flow through either channel. Current occlusion was observed at V_hs between −70 and −10 mV when the I_{ATP} and ACh-induced current (I_{ACh}) were inward, but no occlusion was observed when these currents were outward at a V_h of +40 mV. The I_{ATP} was not inhibited by co-application of ACh when the I_{ACh} was markedly decreased either by removal of permeant cations, by setting V_h close to the equilibrium potential of I_{ACh}, or by the addition of *d*-tubocurarine or serotonin. These results suggest that the inhibitory interaction is attributable to inward current flow of cations through the activated P2XR- and nAChR-channels.

Keywords ATP · ACh · cytosolic Ca^{2+} concentration · Fura-2 microfluorometry · negative interaction between nicotinic and P2X channels · whole-cell patch-clamp recording

M. Sorimachia (✉) · M. Wakamoria · N. Akaikeb
Department of Physiology, Graduate School of Medical and Dental Sciences, Kagoshima University, Kagoshima, 890-8520, Japan
e-mail: ciliary@m.kufm.kagoshima-u.ac.jp

Research Division for Life Sciences,
Kumamoto Health Science University, Kumamoto, 861-5598, Japan

Introduction

The rat area postrema (AP) is a medullary circumventricular organ located in the hindbrain at the level of the obex, with a dense vascular supply devoid of a blood–brain barrier. The lack of a blood–brain barrier makes the AP ideally placed to act as a chemosensitive trigger zone involved in the control of vomiting in response to circulating emetic substances (Borison [1, 2]). Neurons in the AP are also responsive to changes in osmolarity or sodium concentration (Franchini et al. [3]), and can be activated by circulating vasoactive peptides such as angiotensin II (Fink et al. [4]), and arg-vasopressin (Undesser et al.

[5]). Anatomical studies have revealed that the AP sends dense efferent projections to the nucleus tractus solitarius, parabrachial nucleus, nucleus ambiguus, and the dorsal motor nucleus of the vagus, and receives afferent inputs from the hypothalamic paraventricular and dorsomedial nucleii, and from the caudal nucleus tractus solitarius (Morest [6]; Kooy and Koda [7]; Shapiro and Miselis [8]). Thus, the AP is not only capable of responding to circulating hormones, but is also anatomically well situated to regulate a range of other central neurons, including those important in cardiovascular control (Sun and Spyer [9]). The low intrinsic firing rates of AP neurons *in vivo* (Papas et al. [10]) suggests that understanding and modulating excitatory inputs to AP could be particularly important in the functional output of AP neurons. A number of transmitters can evoke excitatory currents in the AP. Inward currents and increases in cytosolic Ca^{2+} ($[Ca]_{in}$) via non-NMDA-glutamate receptors have been reported in rabbit and rat AP neurons, respectively (Jahn et al. [11]; Hay and Lindsley [12]). Our preliminary reports indicated that ATP also induces inward currents and $[Ca]_{in}$ increases via the activation of P2X receptor (P2XR) in isolated rat AP neurons (Sorimachi et al. [13, 14]). In addition, pre- and post-synaptic nicotinic ACh receptors (nAChR) have been demonstrated in the AP in rat brain slices (Funahashi et al. [15]), and we have recently reported the presence of nAChRs in dissociated rat AP neurons (Sorimachi and Wakamori [16]). During that study, we also noticed that many of these AP neurons also responded to ATP, which has prompted us to further investigate ATP responses in AP neurons, and potential interactions between nAChR and P2XR responses. In a variety of different peripheral neurons, including sympathetic neurons of bullfrog (Akasu and Koketsu [17]), rat (Nakazawa et al. [18]), and guinea-pig (Searl et al. [19]), cultured guinea-pig enteric and submucosal neurons (Zhou and Galligan [20] Barajas-Lopez et al. [21]), a negative interaction between P2XR- and nAChR responses has been reported. Such an interaction has also been observed for recombinant P2X2 and α3β4 nAChR channels in Xenopus oocytes and HEK cells (Khakh et al. [22, 23]; Boue-Grabot et al. [24]), where it has been recently suggested that this results from direct physical interactions between co-localized receptors (Khakh et al. [23]). In this study we more fully describe P2XR responses in AP neurons, demonstrate cross-inhibition between P2XRs and nAChRs and characterize some of the features of this cross-inhibition.

Experimental procedures

Preparation of AP neurons

The study was approved by the Committee on Animal Experimentation, Kagoshima University. Wistar rats (13–18 days-old) were anaesthetized with ether and decapitated. The brain was quickly removed from the skull and placed in ice-cold HEPES-buffered saline containing 150 mM NaCl, 5 mM KCl, 2 mM $CaCl_2$, 1 mM $MgCl_2$, 10 mM HEPES and 5.5 mM glucose. The pH of the saline solution was adjusted to 7.4 by adding tris (hydroxymethyl) aminomethane. The brain was sliced at a thickness of 400 μm with a microslicer (DTK-1000, Dosaka, Kyoto, Japan), and the slices were kept in bicarbonate-buffered saline bubbled continuously with 95% O_2–5% CO_2 at room temperature (21–26 °C). The bicarbonate-buffered saline contained 120 mM NaCl, 5 mM KCl, 2 mM $CaCl_2$, 1 mM $MgCl_2$, 20 mM $NaHCO_3$, 2 mM KH_2PO_4 and 5.5 mM glucose. Following 30–60 min incubation, the slices were treated with pronase (0.2 mg/ml) in bicarbonate-buffered saline for 20 min at 33 °C, followed by incubation for 30 min with bicarbonate-buffered saline containing thermolysin (0.12–0.15 mg/ml). The bilateral AP regions were identified with a binocular microscope (Zeiss, Germany), and were cut out using the tip of an injection needle, and subsequently mechanically triturated with fire-polished glass pipettes of decreasing diameters. Dissociated neurons were placed on to the bottom of 35 mm culture dishes (Falcon, USA) for electrophysiological recordings, or on to glass coverslips (Matsunami, Japan) coated with poly-L-lysine for $[Ca]_{in}$ measurements.

Electrophysiological recordings

Electrical measurements were done using the whole-cell patch-clamp recording configuration under voltage-clamp conditions. Patch pipettes were fabricated from borosilicate glass tubes in five or six stages using a pipette puller (Model P-97, Sutter Instrument, San Rafael, CA, USA). The resistance between the recording electrode filled with the internal solution, and the reference electrode in the external solution, was 3–6 MΩ. Ionic currents were measured, and voltages controlled, using a patch-clamp amplifier (EPC-9, Heka, Darmstadt, Germany). All experiments were carried out at 24–26 °C. Culture dishes were placed on an inverted microscope (TE200, Nikon, Japan), and drugs were rapidly applied to single cells using a Y-tube perfusion device. The internal solution (patch

pipette solution) contained 70 mM K-gluconate, 50 mM KCl, 10 mM NaCl, 0.5 mM $CaCl_2$, 3 mM $MgCl_2$, 10 mM HEPES, 10 mM EGTA, and 2 mM ATP. The pH was adjusted to 7.2 with KOH. For measuring current–voltage (*I–V*) relationships, a Cs-based internal solution was employed, which contained 98 mM CsOH, 40 mM CsCl, 98 mM aspartate, 2 mM $MgCl_2$, 5 mM HEPES, 5 mM EGTA, and 2 mM ATP. pH was adjusted to 7.2 with CsOH. The external solution was the HEPES-buffered saline, pH7.4, described above. When *N*-methyl-D-glucamine ($NMDG^+$) or sucrose was substituted for external Na^+ or NaCl, respectively, the osmolarity of the solution was kept constant as measured using an osmometer (Vogel OM801, Germany). To obtain the Ca^{2+}/Na^+ permeability ratio (P_{Ca}/P_{Na}), we measured the reversal potential of the ATP-activated current (E_{ATP}) in the presence of 1 or 110 mM of external Ca^{2+} by stepping the holding potential (V_h) between 10 and 30 mV, using increments of 10 mV. The 1 and 110 mM Ca^{2+} solutions contained 155 or 0 mM NaCl, respectively, in addition to 10 mM HEPES with pH adjusted to 7.4 with NaOH or $Ca(OH)_2$, respectively. The values of P_{Ca}/P_{Cs} and P_{Na}/P_{Cs} were calculated using the constant field equation as described by Lewis ([25]), taking the activity coefficients of Na^+, Cs^+, and Ca^{2+} as 0.75, 0.75, and 0.3, respectively.

Measurement of $[Ca]_{in}$

Dissociated AP neurons on a glass coverslip were incubated with 1–2 μM fura-2 acetoxymethyl ester (fura-2/AM), 0.1% dimethyl sulfoxide, and 1% bovine serum albumin for 45 min at 37 °C. The coverslips were then mounted in a superfusion chamber and placed on the stage of an inverted microscope (Diaphot-TMD, Nikon, Japan). Cells were continuously superfused at a rate of 1 ml/min with HEPES-buffered saline at 24–26 °C via a polyethylene tube placed 1–2 mm away from the cells.

Cells were viewed with a 40× Fluor objective lens (Nikon), and a single cell (10–12 μm diameter) was fixed in a window positioned between the photomultiplier and the microscope. The changes in fluorescence ratios at 340 and 380 nm excitation wavelengths were measured using a CAM-200 spectrometer (Jasco, Japan). The absolute value of $[Ca]_{in}$ was calculated using the formulae as given by Grynkiewicz et al. [26]: $[Ca]_{in} = b \times Kd(R - R_{min})/(R_{max} - R)$. Calibration constants were determined in separate experiments with the same experimental set-up, as described previously (Sorimachi et al. [27]).

Student's paired t test was used to evaluate differences between mean values obtained from the same cells, and Student's unpaired t test was used for data obtained from different groups of cells.

Reagents

The following reagents were used: Fura-2/AM [Dojindo, Kumamoto, Japan], ACh [Horai Chem. Co., Japan], PPADS (pyridoxal-phosphate-6-azophenyl-2′, 4′-disulphonic acid) [RBI, USA.], pronase [Calbiochem., USA], thermolysin, ATP, 2-methylthio-ATP, ATPγS, α,β-methylene-ATP, β,γ-methylene-ATP, ADP, nitrendipine, nicardipine, suramin [all from Sigma, Aldrich, Tokyo, Japan], ω-conotoxin-MVIIA, ω-conotoxin-MVIIC and ω-agatoxin-IVA [all from Peptide Institute, Osaka, Japan].

Results

ATP-induced current

Rapid application of ATP (100 μM) to isolated AP neurons voltage clamped at a V_h of −70 mV induced an inward current, which desensitized slowly (Fig. 1A). The ATP-induced current (I_{ATP}) was recorded at various V_hs between −70 and +50 mV (Fig. 1: N = 6), and the relative current amplitude was plotted against V_h exhibiting a strong inward rectification. The E_{ATP}, estimated from the intersection of the current response and the zero voltage-axis (Fig. 1B), was 22.7 ± 0.9 mV (N = 18).

To investigate the ATP concentration-response relationship, care was taken to adjust the pH of the solutions containing higher concentrations of ATP to 7.3, since addition of ATP reduced pH and a small decrease in pH to 7.1 increased the I_{ATP} to 189 ± 8% (N = 6) of control (pH7.3), as previously reported for recombinant $P2X_2$ receptors (King et al. [28]). The responses to different ATP concentrations were flanked by responses to the control concentration of 100 μM, and normalized responses were expressed relative to the average of these control responses (Fig. 1C; Ca2mM). We also examined the effects of 0.1 and 10 mM Ca^{2+} on I_{ATP}. As summarized in Fig. 1C, an increase in the external concentration of Ca^{2+} shifted the concentration-response curve for ATP to the right, with the half-maximum effective concentration (EC_{50}) values at 0.1, 2 and 10 mM Ca^{2+} being 30, 70, and 190 μM, respectively.

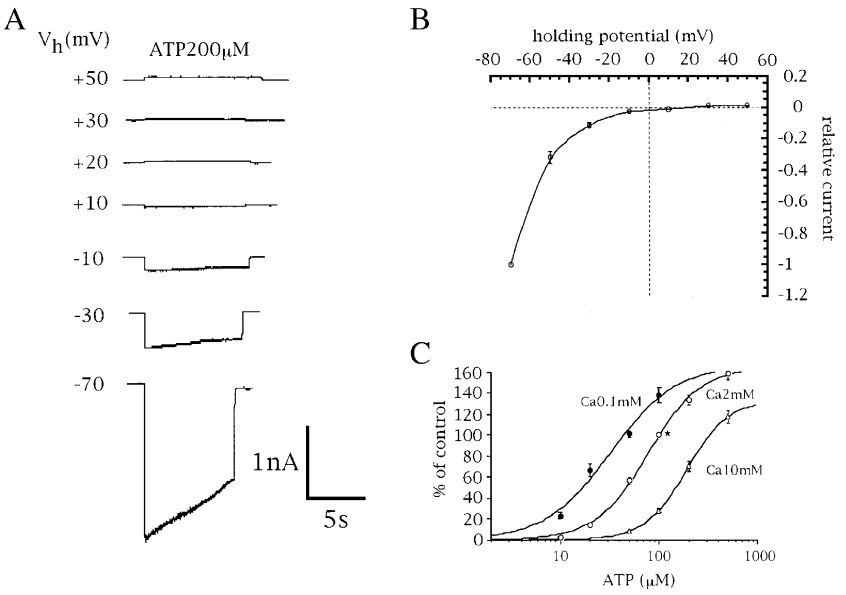

Fig. 1 Current–voltage relationship for ATP-induced currents. **A**) Representative currents in response to 200 μM ATP recorded at V_hs between −70 and +50 mV. **B**) Current–voltage relationship for the I_{ATP}. All responses are normalized to the peak current amplitude obtained at a V_h of −70 mV, and each point is the mean ± S.E.M. of five neurons. **C**) Averaged concentration–current relationships for ATP in the presence of 0.1, 2, and 10 mM external Ca^{2+}. All responses were normalized to the mean of two control responses induced by 100 μM ATP in saline containing 2 mM external Ca^{2+} before and after the test response. Each point is the average ± S.E.M of responses from four to six neurons.

The purinergic agonists, 2-methylthio-ATP (50 μM) and ATPγS (50 μM) induced currents that were 41 ± 3% (N = 4), and 41 ± 4% (N = 5), respectively, of the I_{ATP} in response to 100 μM ATP. ADP (0.5 mM) did not produce any response. The I_{ATP} in response to 50 μM ATP was inhibited by the P2 antagonists; suramin (10 μM and 20 μM) and PPADS (50 μM), with the response being 35 ± 2% (N = 5), 25 ± 2% (N = 4), and 56 ± 5% (N = 5), of the control I_{ATP}, respectively.

ATP-induced $[Ca]_{in}$ increase

ATP also increased $[Ca]_{in}$ in a dose-dependent manner (Fig. 2A). These responses were all recorded in the presence of 2 mM external Ca^{2+}, and the $[Ca]_{in}$ increases by various concentrations of ATP were normalized to that induced by 100 μM ATP. The normalized and averaged responses to ATP, 2-methylthio-ATP and ATPγS are shown in Fig. 2B. There was no ATP-induced $[Ca]_{in}$ increase in the absence of external Ca^{2+} (N = 6; data not shown). Furthermore, neither ADP, α,β-methylene-ATP nor β,γ-methylene-ATP increased $[Ca]_{in}$ when tested at concentrations of 200 μM(data not shown). The ATP-induced $[Ca]_{in}$ increases were inhibited by suramin and PPADS (Table 1).

Effects of Ca^{2+} channel antagonists on ATP-induced $[Ca]_{in}$ increase

Previous results, using cultured rabbit AP neurons, demonstrated the presence of a ω-conotoxin-M C-sensitive Ca^{2+} response, but that did not involve L- or N-type Ca^{2+} channels (Hay et al. [29]). We also investigated the effects of various Ca^{2+} channel antagonists on $[Ca]_{in}$ increases induced by high KCl (110 mM) and ATP (100 μM). Antagonist for the L-type (nitrendipine, nicardipine), N-type (ω-conotoxin-M A), or P/Q-type (ω-conotoxin-M C) Ca^{2+} channels each substantially inhibited these $[Ca]_{in}$ increases (Table 1). In contrast, the selective P-type Ca^{2+} channel antagonist, ω-agatoxin IVA (1 μM), did not have any inhibitory effect on the $[Ca]_{in}$ increases (98 ± 5% of control, N = 4).

ATP-induced current in the absence of external Na^+

When external Na^+ was completely replaced by $NMDG^+$, and in the absence of external Ca^{2+} (0 Ca^{2+} plus 0.5 mM EGTA), the I_{ATP} was markedly reduced to 8 ± 1% of the control I_{ATP} recorded in the presence of external Ca^{2+} and 150 mM Na^+ (N = 9, Fig. 3A). This current was further reduced to 4 ± 1% (N = 3) in the presence of 20 μM suramin. The small

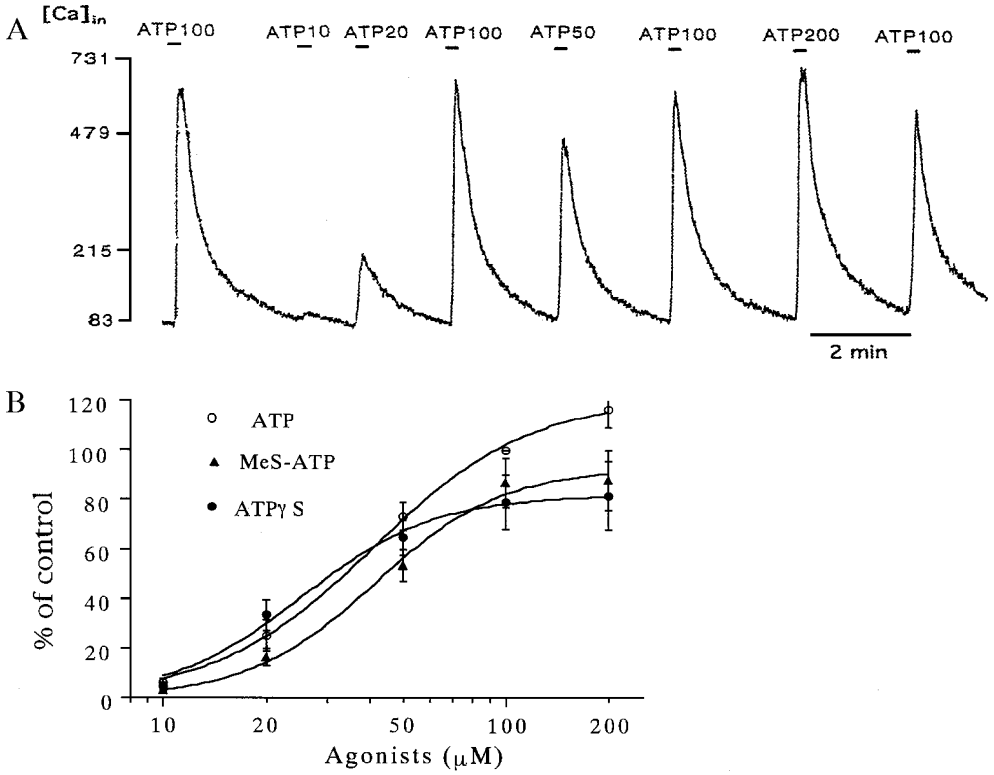

Fig. 2 Concentration-response relationships for the $[Ca]_{in}$ increases in response to ATP and ATP analogues. **A**) Representative $[Ca]_{in}$ increases induced by various concentrations of ATP in the presence of 2 mM external Ca^{2+}. **B**) Averaged concentration–response relationships for ATP and ATP analogues. All responses were normalized to the mean of two control responses induced by 100 μM ATP before and after the test response. Each point is the mean ± S.E.M. of data from five to nine neurons. MeS-ATP: 2-methylthio-ATP.

Table 1 Effects of P2 receptor antagonists and Ca^{2+} channel blockers on the $[Ca]_{in}$ increases induced by ATP and high K^+-saline

Stimulus	Blockers	Percent of control
ATP100 M	Suramin 10 M	55 ± 7 (*N* = 5)
	20 M	30 ± 5 (*N* = 6)
	50 M	13 ± 3 (*N* = 5)
	PPADS 10 M	96 ± 6 (*N* = 3)
	20 M	70 ± 8 (*N* = 9)
	50 M	25 ± 5 (*N* = 6)
	100 M	11 ± 5 (*N* = 4)
110 mMKCl	Nitrendipine 2 M	44 ± 4 (*N* = 16)
	−CT.M C 2 M	61 ± 4 (*N* = 16)
	−CT.M A 2 M	62 ± 6 (*N* = 16)
	−CT.M A 2 M + −CT.M C 2 M	58 ± 5 (*N* = 10)
ATP100 M	Nitrendipine 2 M	56 ± 4 (*N* = 21)
	Nicardipine 2 M	47 ± 9 (*N* = 10)
	Cd^{2+} 50 M	27 ± 3 (*N* = 14)
	−CT.M A 2 M + −CT.M C 2 M	77 ± 9 (*N* = 4)

The mean $[Ca]_{in}$ increase induced by the first and third applications of ATP (100 μM) or 110 mM KCl were averaged and referred to as 100%, and the response in the presence of the P2 antagonist or Ca^{2+} channel blocker was expressed as a percentage of this control value. The cell was pre-treated for 30 s with the indicated agent before the second stimulation with 100 μM ATP or 110 mM KCl. Number of experiments is shown in parentheses. ω-CT ω-conotoxin.

suramin-sensitive, Na^+-independent current supports the previous suggestion that the P2XR channel is permeable to glucosamine (Nakazawa [30]). To confirm this, ATP did not induce a current at all when sucrose (0.25 M) was substituted for NaCl (again in the absence of external Ca^{2+}, $N = 5$). Addition of Ca^{2+} to the $NMDG^+$- substituted saline further increased I_{ATP}. The currents induced by 500 μM ATP in the presence of 2 and 10 mM Ca^{2+}, but in the absence of external Na^+ (replaced by $NMDG^+$) were 18 ± 2% ($N = 11$) and 29 ± 2% ($N = 14$, Fig. 3B) of the control I_{ATP}, respectively. Similarly, the currents induced by 500 μM ATP in the presence of 2 and 10 mM Ca^{2+} added to the sucrose-substituted saline were 6 ± 1% ($N = 6$), and 13 ± 2% ($N = 16$; Fig. 3C) of the control I_{ATP}, respectively.

We also measured the E_{ATP} of I_{ATP} in the presence of 1 mM external Ca^{2+} and 150 mM NaCl or 110 mM external Ca^{2+} and 0 mM NaCl. The E_{ATP} at 110 mM Ca^{2+} was 21.1 ± 1.0 mV ($N = 18$), from which we calculated a P_{Ca}/P_{Cs} of 6.3. The E_{ATP} at 1 mM Ca^{2+} was 20.2 ± 1.0 mV ($N = 13$), from which we calculated a P_{Na}/P_{Cs} ratio of 2.1. From these, we obtained a P_{Ca}/P_{Na} ratio of 3.0, confirming the substantial Ca^{2+} permeability of P2XRs.

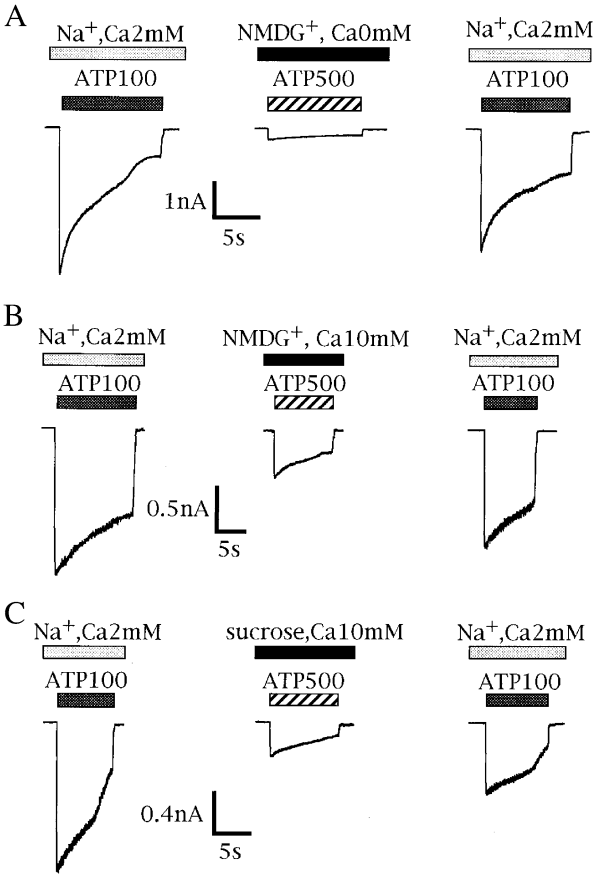

Fig. 3 ATP-induced current in Na^+- and NaCl-free saline containing 0 and 10 mM Ca^{2+}. **A**) A representative I_{ATP} recorded in Na^+-free (Na^+ replaced by $NMDG^+$) and Ca^{2+}-free saline (containing 0.5 mM EGTA) at a V_h of −70 mV. **B**) A representative I_{ATP} in Na^+-free ($NMDG^+$) saline containing 10 mM Ca^{2+}. **C**) A representative I_{ATP} in NaCl-free (NaCl replaced by sucrose) saline containing 10 mM Ca^{2+}.

Negative interaction between P2XR and nAChR channels

Requirement of actual current flow through receptor channels for cross-inhibition.

It has previously been reported that there is mutual occlusion between P2XR and nAChR in some neurons (Nakazawa et al. [18]; Nakazawa [30]; Searl et al. [19]; Zhou and Galligan [20]; Barajas-Lopez et al. [21]; Khakh et al. [22, 23]; Boue-Grabot et al. [24]). To examine whether there were negative interactions between the ACh-activated current (I_{ACh}) and I_{ATP}, one receptor agonist was added in the presence of the other. As shown in Fig. 4A, the I_{ACh} (100 μM) was markedly reduced when activated in the presence of ATP (50 μM). We next examined I_{ACh} (100 μM) in the presence of various concentrations of ATP. With 2, 10, 20, and 100 μM ATP, I_{ACh} was reduced to 95 ± 1% ($N = 20$), 84 ± 2% ($N = 24$), 60 ± 4% ($N = 15$), and 46 ± 6% ($N = 7$), respectively, of control ($P < 0.01$ except at 2 μM ATP). Thus, the I_{ACh} inhibition became stronger as the concentration of ATP was increased and with a higher agonist-receptor occupancy. In fact, when I_{ATP} at 100 μM ATP was markedly inhibited in the presence of 200 μM PPADS (8 ± 2% of control, $N = 6$), I_{ACh} was not occluded (97 ± 1% of control; $N = 6$). When the peak amplitude of I_{ATP}, evoked by various concentrations of ATP, was plotted against the ratio of I_{ACh} in the presence and absence of ATP, there was an inverse correlation between the amplitudes of these responses (Fig. 4B). Conversely, when ATP (50 μM) was applied in the presence of ACh (100 μM), I_{ATP} was also occluded (Fig. 4C). Again, when I_{ACh} at 200 μM ACh was nullified in the presence of 1 mM hexamethonium, a nAChR antagonist (0.2 ± 0.2% of control, $N = 6$), I_{ATP} was 96 ± 2% ($N = 6$) of control. I_{ACh} at 10, 20, 50, and 200 μM ACh were 6 ± 2% ($N = 5$), 20 ± 4% ($N = 5$), 61 ± 8% ($N = 6$), and 139 ± 8% ($N = 6$) of I_{ACh} at 100 μM. There was also an inverse correlation between the peak amplitude of I_{ACh}, evoked by various concentrations of ACh, and the ratio of I_{ATP} in the presence and absence of ACh (Fig. 4D). However, the inhibition of I_{ATP} by nAChR activation was weaker than that of I_{ACh} by P2XR activation. As the I_{ACh} desensitized faster than the I_{ATP}, the weaker inhibition of I_{ATP} by ACh could be

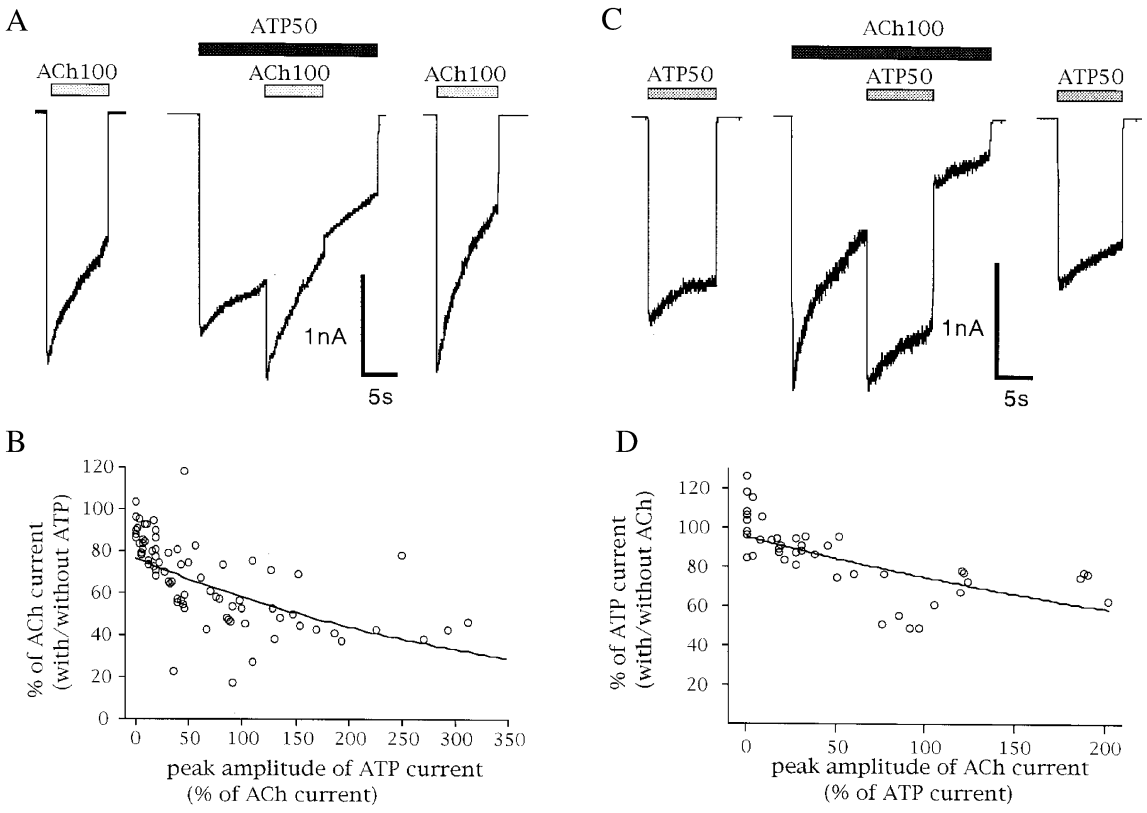

Fig. 4 Inhibition of I_{ACh} and I_{ATP}, respectively, in the presence of ATP and ACh. **A**) Sample currents in response to ACh (100 μM) in the presence of ATP (50 μM). The responses to ACh applied in the presence of ATP were reduced. The extent of occlusion was normalized to the control ACh responses recorded before and after ATP application. This sequence was routinely repeated twice or three times, and the averaged amount of occlusion was plotted in **B**. **B**) Relative amplitude of the ACh current amplitude in the presence of ATP (*ordinate*) plotted against the peak amplitude of I_{ATP} obtained in the same neuron (*abscissae*). Note the negative correlation between these two variables. The line was drawn using KaleidaGraph (Synergy Software). V_h: −70 mV. **C**) The I_{ATP} was recorded in the presence of 100 μM ACh and this response was flanked by control ATP alone responses. This sequence was routinely obtained twice or three times in the same cell, and the averaged amount of occlusion was plotted in **D**. **D**) The ratio of the ATP current amplitude in the presence and absence of ACh (*ordinate*) is negatively correlated with the peak amplitude of I_{ACh} (*abscissae*). V_h : −70 mV.

due to the reduced amplitude of the I_{ACh} at the time of ATP application.

To examine this possibility, I_{ATP} was measured in the presence of both ACh and d-tubocurarine (dTc, 10 μM) or serotonin (5HT, 50 μM), two experimental conditions which change the time course of the I_{ACh} response. The former agent, dTc, has been shown to be both an open channel blocker and a competitive antagonist of nAChR (Manalis [31]), and, as expected, a low concentration (10 μM) slightly reduced the peak amplitude of I_{ACh} (79 ± 4% of control, N = 11) and caused the I_{ACh} to be terminated within 0.5 s (Fig. 5A, insert). Once the I_{ACh} response had returned to baseline (in the presence of ACh and 10 μM dTc) and ATP was applied, there was no inhibition of I_{ATP} (95 ± 1% of control, N = 5; Fig. 5A). The I_{ATP} in the presence of ACh alone was 77 ± 4% of control (N = 5, P < 0.01; Fig. 5A). When we measured the current ($I_{ACh+ATP+dTc}$) induced by a combination of ACh, ATP and dTc, the peak amplitude of $I_{ACh+ATP+dTc}$ was occluded under these conditions, being 74 ± 2% (N = 10) of the predicted sum of I_{ATP} and $I_{ACh+dTc}$ (Fig. 5B). The level of $I_{ACh+ATP+dTc}$ at 0.5 s following ligand application, which corresponds to a time when the nAChR channels are completely blocked (Fig. 5A, insert), was 96 ± 3% (N = 8) of the control I_{ATP}, measured immediately before and after (Fig. 5C). These results suggest that the inhibition of I_{ATP} by I_{ACh} disappears immediately after the I_{ACh} is abolished, although ACh is still present and bound to the nAChRs. 5HT has been shown to also accelerate the decay of I_{ACh} (Grassi et al. [32]; Garcia-Colunga and Miledi [33]; Sorimachi and Wakamori [34]), but not to the same extent as dTc. 5HT at 50 μM decreased the peak amplitude of I_{ACh} slightly, to 88 ± 4% (N = 6) of control, and reduced the time constant (tau) of I_{ACh} decay from 2.02 ± 0.18 to 1.06 ± 0.19 s (N = 6). As shown in Fig. 5D, the extent of inhibition of I_{ATP} by

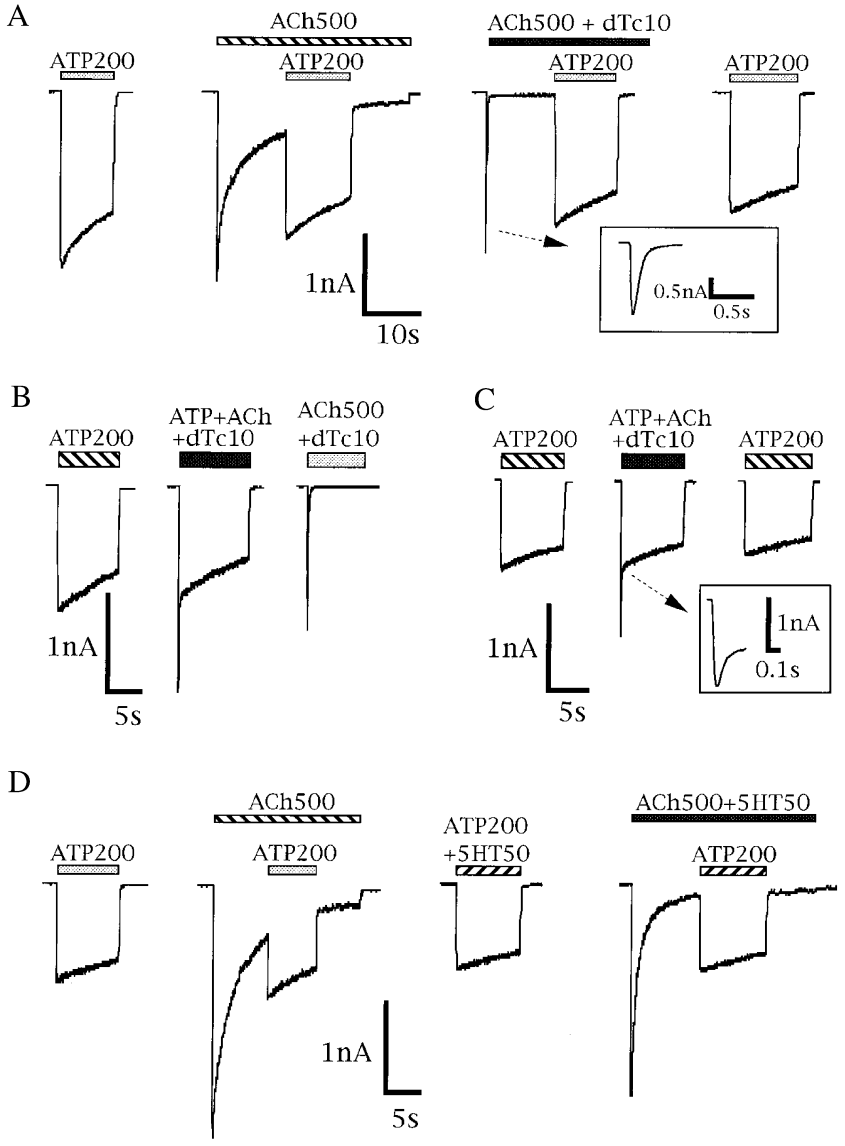

Fig. 5 Loss of the inhibition of I_{ATP} by ACh in the presence of dTc and 5HT. **A**) Representative I_{ATP} in control conditions (applied alone), in the presence of ACh and in the presence of ACh and dTc. This sequence was routinely repeated twice, and the averaged response was obtained. Note the very transient nature of I_{ACh} in the presence of dTc, with the current returning to baseline levels within 0.5 s (insert). Note also the lack of occlusion under these conditions. V_h: −70 mV. **B**) Effect of dTc on $I_{ACh+ATP}$. The sequence of applications was repeated multiple times in each neuron. The peak amplitude of $I_{ACh+ATP+dTc}$ was smaller than the predicted sum of I_{ATP} and $I_{ACh+dTc}$. **C**) Rapid recovery of I_{ATP} from inhibition by ACh in the presence of dTc. The amplitude of $I_{ACh+ATP+dTc}$ 0.5 s following application was equal to the mean of two control I_{ATP} at an equivalent time. Inset shows the rapid decline of $I_{ACh+ATP+dTc}$ on an expanded time scale. **D**) Representative I_{ATP} in control conditions, in the presence of ACh, and in the presence of both ACh and 5HT. In this example, the tau of I_{ACh} in response to the first application was 2.7 s, while the tau of $I_{ACh+5HT}$ was 0.9 s, showing the acceleration of the I_{ACh} decay by 5HT. Note the reduced occlusion under these conditions. V_h : −70 mV.

ACh was smaller (to 92 ± 2% of control, $N = 6$) in the presence of ACh and 5HT compared to that in the presence of ACh alone (to 73 ± 3% of control, $N = 6$; $P < 0.01$).

Next, we measured the current induced by the concomitant applications of ACh and ATP ($I_{ACh+ATP}$) at a V_h of −70 mV. As shown in Fig. 6A, $I_{ACh+ATP}$ was 75 ± 1% ($N = 44$; $P < 0.01$) of the predicted sum of I_{ACh} and I_{ATP}. The decay phase of I_{ACh}, I_{ATP} and $I_{ACh+ATP}$ were fit to a single exponential function, giving tau of 3.0 ± 0.2, 7.5 ± 0.6 and 3.7 ± 0.2 s, respectively. When the decay of I_{ACh} was accelerated by the presence of 100 μM 5HT, the tau of I_{ACh}, I_{ATP}, and $I_{ACh+ATP}$ were 0.8 ± 0.3 s ($N = 7$), 7.4 ± 1.4 s ($N = 7$) and 2.6 ± 0.8 s ($N = 7$), respectively (the amplitude of $I_{ACh+ATP}$ under these conditions was 76 ± 2% of the predicted sum of I_{ACh} and I_{ATP}). Thus, $I_{ACh+ATP}$ desensitization occurs with kinetics that cannot be

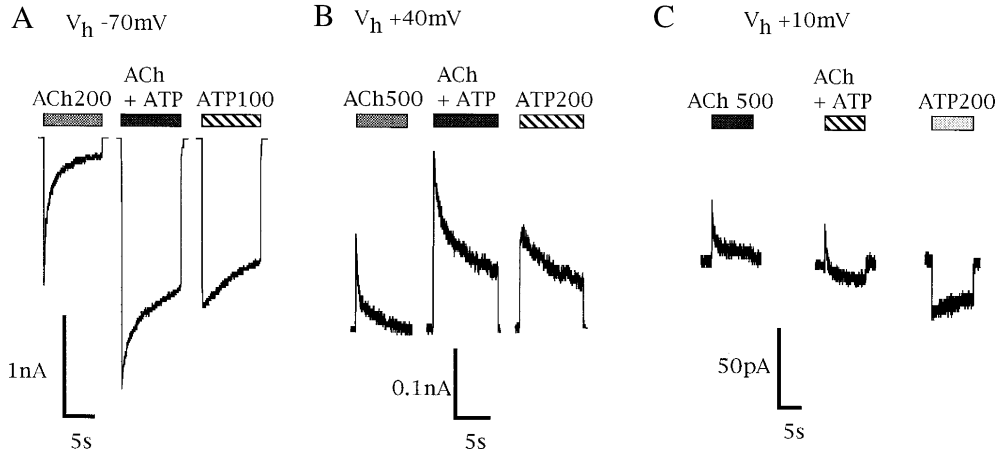

Fig. 6 Voltage dependence of I_{ACh} and of I_{ATP} occlusion. **A**) At a V_h of −70 mV, co-application of ACh (200 μM) and ATP (100 μM) induced an inward current that was smaller in amplitude than the predicted sum of the individual I_{ACh} and I_{ATP}. **B**) At a V_h of +40 mV, the amplitude of the outward current induced by the co-application of ACh (500 μM) and ATP (200 μM) was equal to the predicted sum of the individual I_{ACh} and I_{ATP}. **C**) Co-application of ATP and ACh does not markedly change E_{ACh} or E_{ATP}. Representative currents induced by ACh, ATP, and by co-application of ACh and ATP at a V_h of +10 mV. Note that $I_{ACh+ATP}$ is composed of early outward and delayed inward current, corresponding to the ACh component and the ATP component, respectively.

explained by the desensitization kinetics of I_{ACh} or I_{ATP} alone, suggesting that $I_{ACh+ATP}$ is mediated via both receptors.

When Ca^{2+} was omitted from extracellular solution, the negative interaction between the two receptor channels was still obtained; with $I_{ACh+ATP}$ being 77 ± 1% ($N = 5$; $P < 0.01$) of the predicted sum of I_{ACh} and I_{ATP}. Hence negative interaction is not mediated by a Ca^{2+} influx-dependent mechanism, although both nAChR and P2XR are Ca^{2+}-permeable cation channels (Fieber and Adams [35]; Rogers and Dani [36]). This result, however, does not necessarily rule out the possible involvement of $[Ca]_{in}$ in negative interaction.

Occlusion was not only observed at a V_h of −70 mV; $I_{ACh+ATP}$ at V_hs of −20, and −10 mV were 80 ± 2% ($N = 12$; $P < 0.01$), and 76 ± 2% ($N = 8$; $P < 0.01$), respectively, of the predicted sum of I_{ACh} and I_{ATP}. In sharp contrast, such occlusion was not observed at a positive potential; the outward current caused by co-application of ACh and ATP at a V_h of +40 mV was 100 ± 1% ($N = 10$) of the predicted sum of individual current (Fig. 6B).

We next investigated the possibility that the combined addition of ACh and ATP alters the driving force for Na^+, by attempting to measure $E_{ACh+ATP}$. In these studies, currents in response to ACh, ATP and both ligands were measured at various fixed potentials close to the reversal potential for I_{ACh} and I_{ATP}. The E_{ACh} and E_{ATP} were 8.7 ± 1.5 mV ($N = 5$) and 21.0 ± 1.6 mV ($N = 7$), respectively, and $I_{ACh+ATP}$ measured at a potential between these two reversal potentials (e.g.10 mV, Fig. 6C) showed a combination of both the ACh-induced outward current and the ATP-induced inward current. These results suggest that the driving force for permeant ions during combined ACh and ATP is similar to that during the application of each ligand separately.

The question arises as to whether occlusion is specific just for Na^+ ions or whether inward currents carried by cations other than Na^+ can also contribute to occlusion during co-activation of nAChRs and P2XRs. To address this question, we measured I_{ACh}, I_{ATP}, and $I_{ACh+ATP}$ in the presence of Na^+-free ($NMDG^+$) saline containing 10 mM Ca^{2+} (Fig. 7). $NMDG^+$ does not permeate through nAChR (Sorima-

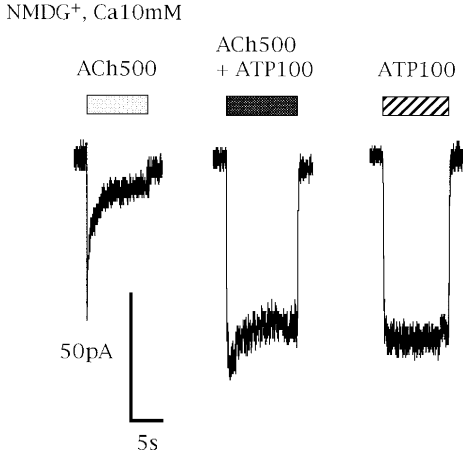

Fig. 7 Occlusion of $I_{ACh+ATP}$ in the presence of Na^+-free saline containing 10 mM Ca^{2+}. I_{ACh}, I_{ATP} or $I_{ACh+ATP}$ was recorded 20 s after switching to Na^+-free (replaced by $NMDG^+$) saline containing 10 mM Ca^{2+}. The sequence of applications was repeated multiple times. Following each ligand application, the external solution was changed back to normal saline containing 150 mM Na^+ before the next ligand application. V_h: −70 mV.

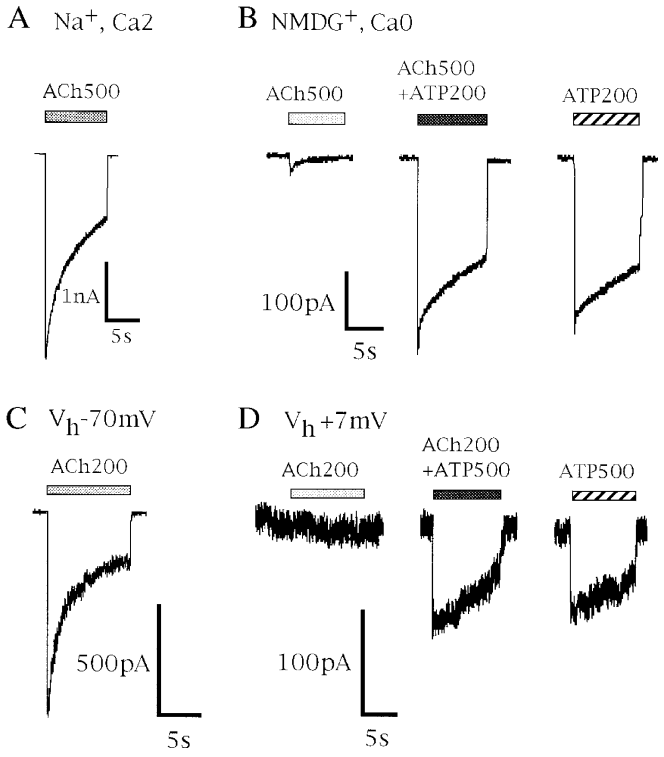

Fig. 8 Lack of inhibition in response to co-application of ACh and ATP under two experimental conditions designed to virtually eliminate I_{ACh}. **A**) Control I_{ACh} recorded at a V_h of −70 mV in standard saline. **B**) Current responses recorded at −70 mV from 20 s after exchanging the standard saline for a Na^+-free (replaced by $NMDG^+$), Ca^{2+}-free saline. This sequence was repeated twice or three times. Note the small amplitude of I_{ACh}, and the lack of occlusion of $I_{ACh+ATP}$. **C**) Control I_{ACh} recorded at a V_h of −70 mV in another neuron. **D**) Representative traces of I_{ACh}, I_{ATP}, and $I_{ACh+ATP}$ recorded at a V_h of +7 mV, which is very close to E_{ACh}. Note the lack of occlusion at this potential, when current flow through the AChR is negligible.

chi and Wakamori [16]), and hence I_{ACh} would be mediated by only Ca^{2+} influx, whereas I_{ATP} would be mediated via both $NMDG^+$ and Ca^{2+} influx (Fig. 3). Under these conditions, $I_{ACh+ATP}$ was again occluded, being 70 ± 3% of the predicted sum of I_{ACh} and I_{ATP} (N = 11; $P < 0.01$; Fig. 7).

In a further attempt to distinguish whether channel activation or ion permeation was primarily responsible for occlusion of one channel by the other, we compared I_{ATP} with $I_{ACh+ATP}$ under two experimental conditions, in which a higher concentration of ACh should activate nAChR but produce very little current. In the absence of Na^+ and Ca^{2+} (replaced by $NMDG^+$) application of ACh induces a negligible current (Sorimachi and Wakamori [16]), while ATP induces a substantial current under the same conditions (Fig. 3A). As shown in Fig. 8B, there was no occlusion in these conditions; the amplitude of $I_{ATP+ACh}$ was 105 ± 1% (N = 10) of the predicted sum of I_{ATP} and I_{ACh}. We also investigated currents in response to the ligands at a potential close to the E_{ACh} (7 ± 2 mV in this experiment, N = 13), taking advantage of the more positive E_{ATP} (22.7 ± 0.9 mV), so that at this potential only the I_{ATP} was observed. The amplitude of $I_{ATP+ACh}$ was 105 ± 3% (N = 13) of that of I_{ATP}, and I_{ACh} was close to zero (Fig. 8D). These results are, however, in contrast to that obtained in sympathetic neurons (Nakazawa[30]), in which I_{ATP} in the absence of both Na^+ (replaced by glucosamine) and Ca^{2+} was inhibited in the presence of ACh, which caused no current (Nakazawa [30]). In these experiments, we only included data in which I_{ATP} was large enough to be clearly resolved, greater than 50 pA (corresponding to a control I_{ATP} at a V_h of −70 mV larger than 1.5 nA). These results suggest that actual current flow through both nAChR and P2XR is responsible for occlusion.

Discussion

In this study, we found that ATP induced an inward current and increased $[Ca]_{in}$ in isolated rat AP neurons. The ATP-induced current and $[Ca]_{in}$ increase were mimicked by ATPγS and 2-methylthio-ATP, but not by α, β-methylene-ATP, β, γ-methylene-ATP nor ADP, and was inhibited by suramin and PPADS, suggesting that it was mediated by P2XRs. These

results are in good agreement with previous histochemical findings, which demonstrated the presence of $P2X_2$, $P2X_4$, and $P2X_6$ receptor mRNAs (Collo et al. [37]), and of $P2X_2$ receptor immunoreactivity in AP neurons (Kanjhan et al. [38]; Atkinson et al. [39]).

The I_{ATP} showed strong inward rectification and the E_{ATP} was 22.7 ± 0.9 mV (Fig. 1B). The amplitude of I_{ATP} varied inversely with the extracellular Ca^{2+} concentrations (Fig. 1C). The inhibitory effect of increasing extracellular Ca^{2+} has also been reported in rat sensory neurons (Krishtal et al. [40]), PC-12 cells (Nakazawa et al. [18]), ventromedial hypothalamic neurons (Sorimachi et al. [41]), and in cells expressing recombinant $P2X_2$ receptors (Evans et al. [42]; Virginio et al. [43]), where an allosteric alteration of the ATP binding sites has been suggested to be the underlying mechanism.

The I_{ATP} was markedly reduced, but still persisted when $NMDG^+$ was substituted for external Na^+ even in the absence of Ca^{2+} (Fig. 3A). Since ATP did not induce a current when sucrose was substituted for external NaCl, our result suggests that $NMDG^+$ could permeate through P2XR. A substantial I_{ATP} has been similarly reported in PC-12 cells and sympathetic neurons when glucosamine was substituted for Na^+ (Nakazawa et al. [18]; Nakazawa [30]). The addition of Ca^{2+} to NMDG-Cl- and sucrose-substituted saline increased the I_{ATP} (Fig. 3B and C, respectively), indicating that Ca^{2+} also permeates through P2XR channel. We quantified the relatively high Ca^{2+} permeability, obtaining a P_{Ca}/P_{Na} ratio of 3.0. A relatively high permeability of P2XR to Ca^{2+} has been reported in previous studies (Nakazawa et al. [18]; Sorimachi et al. [41]; Evans et al. [42]; Virginio et al. [43]). Although direct influx of extracellular Ca^{2+} through P2XR channel may thus contribute to the ATP-induced $[Ca]_{in}$ increase, membrane depolarization and the secondary activation of voltage-dependent Ca^{2+} channels could also make a significant contribution to the $[Ca]_{in}$ increase. In fact, the high K^+- and ATP-induced $[Ca]_{in}$ increases were substantially inhibited by a range of Ca^{2+} channel antagonists, including those which block L- and N-type Ca^{2+} channels (Table 1). This is in contrast to a previous study, which reported an absence of the L- and N-type Ca^{2+} channels in rabbit AP neurons (Hay et al. [12]). The discrepancies between their results and ours could be, at least in part, accounted for by the use of different AP preparations (cultured rabbit neurons *vs.* acutely dissociated rat neurons).

The present results, in combination with our previous demonstration of nAChR on AP neurons (Sorimachi and Wakamori [16]), suggest that both ATP and ACh may act as excitatory neurotransmitters in AP neurons, although their release from presynaptic nerve terminals has not yet been reported. We also report a negative functional interaction between P2XRs and nAChRs in AP neurons, as has been observed in a variety of peripheral neurons and in recombinant expression systems (Nakazawa et al. [18]; Nakazawa [30]; Zhou and Galligan [20]; Barajas-Lopez et al. [21]; Searl et al. [19]; Khakh et al. [22, 23]; Boue-Grabot et al. [24]). This is the first report, that we are aware of, of such interactions occurring in central neurons. When ACh was applied in the presence of ATP, there was a positive correlation between the peak amplitude of inward I_{ATP} and the amount of occlusion of inward I_{ACh} (Fig. 4A and B). The converse was also true when ATP was applied in the presence of ACh (Fig. 4C and D). Non-additivity of the $I_{ACh+ATP}$ was observed even when the inward current was carried by $NMDG^+$ and/or Ca^{2+} (Fig. 7). Co-application of two agonists did not seem to change the driving force for Na^+, because at a V_h between E_{ACh} and E_{ATP} an outward current due to the activation of nAChR, followed by an inward current due to the activation of P2XR, was observed (Fig. 6C). Occlusion was also observed at a V_h of −10 mV, which is closer to E_{ACh} or E_{ATP}. Furthermore, the removal of external Ca^{2+} did not alter the occlusion, and thus a Ca^{2+}-mediated mechanism does not contribute to the current occlusion.

The $I_{ACh+ATP}$ occlusion was observed at all negative holding potentials when the current was inward but was not observed for outward currents at a V_h of +40 mV. Here the outward $I_{ACh+ATP}$ was not different from the predicted sum of I_{ACh} and I_{ATP} (Fig. 6B). The same dependence on current direction has been reported in guinea-pig enteric and submucosal neurons (Zhou and Galligan [20]; Barajas-Lopez et al. [21]), suggesting that the current occlusion was triggered by the inward movement of cations through two channels.

Some investigators have shown that the amplitude of $I_{ACh+ATP}$ is equal to or even smaller than that of either I_{ACh} or I_{ATP}. For instance, the concentration of one agonist causing little or no inward current produced dramatic occlusion of the inward current generated by the other agonist (Searl et al. [19]). Khakh et al. [22] using Xenopus oocytes co-expressing $P2X_2$ and α3β4 nAChR channels, provided several lines of evidence which indicated that occlusion was mostly mediated by the inhibition of the nAChR channel by activation of the P2XR. However, we found that concomitant application of two agonists always caused a larger current than either agonist (Fig. 6A), and that the amount of occlusion of one

channel current in the presence of the other channel agonist was correlated with the amplitude of current through the other channel (Fig. 4). Furthermore, we found that $I_{ACh+ATP}$ desensitizes faster than I_{ATP}, but more slowly than I_{ACh}, and $I_{ACh+ATP}$ at a V_h between E_{ACh} and E_{ATP} showed a combination pattern of early outward I_{ACh} and delayed inward I_{ATP} (Fig. 6C). These results both strongly suggest that in AP neurons, $I_{ACh+ATP}$ are carried through both nAChR and P2XR channels, and that inhibition between these channels is reciprocal.

The I_{ATP} was not inhibited by co-application of ACh when the inward I_{ACh} was markedly reduced in the absence of permeant cations (Fig. 8B) or at a V_h very close to E_{ACh} (Fig. 8D), and the inhibited I_{ATP} in the presence of ACh (Fig. 5B) recovered as soon as the nAChR channel closed in the presence of dTc (Fig. 5C). These results thus suggest that the inhibitory interaction not only requires the activation of both receptor channels, but also requires a substantial current to flow through these channels. These results are in contrast to that obtained in sympathetic neurons, in which the ATP-induced glucosamine influx was inhibited in the presence of ACh (Nakazawa [30]). The cause of this inconsistency remained unknown, but may reflect a real difference in the underlying mechanisms of occlusion in these two types of neurons.

Altogether, our results have characterized the P2XR responses in AP neurons and the cross-inhibition between P2XRs and nAChRs in AP neurons. We show that the current flow through one receptor channel hinders the current flow through the other channel. These interactions support the notion that these channels are positioned very close to each other, as has been previously considered (Zhou and Galligan [20]; Barajas-Lopez et al. [21]; Khakh et al. [22]; Boue-Grabot et al. [24]) and more recently demonstrated for recombinant channels (Khakh et al. [23]). These results will be important to consider when designing ligands to modify excitability of ATP neurons and may have some physiological function during co-activation of P2XRs and nAChRs by synaptically released transmitters.

References

1. Borison HL (1974) Area postrema: Chemoreceptor trigger zone for vomiting is that all? Life Sci 14:1807–1817
2. Borison HL (1984) History and status of the area postrema. Fed Proc 43:2937–2940
3. Franchini LF, Johnson AK, De Olmos J et al (2002) Sodium appetite and Fos activation in serotonergic neurons. Am J Physio 282:R235–243
4. Fink GD, Bruner CA, Mangiapane ML (1987) The area postrema is critical for angiotensin induced hypertension. Hypertension 9:355–361
5. Undesser KP, Hasser EM, Haywood JR et al (1985) Interactions of vasopressin with the area postrema in arterial baroreflex function in conscious rabbits. Circ Res 56:410–417
6. Morest DK (1967) Experimental study of the projections of the nucleus of the tractus solitarius and the area postrema in the cat. J Comp Neurol 130:277–299
7. Kooy VDD, Koda LY (1983) Organization of the projections of a cirumventricular organ: The area postrema in the rat. J Comp Neurol 219:328–338
8. Shapiro RE, Miselis RR (1985) The central neural connections of the area postrema of the rat. J Comp Neurol 234:344–364
9. Sun MK, Spyer KM (1991) GABA-mediated inhibition of medullary vasomotor neurons by area postrema stimulation in rats. J Physiol (Lond) 436:669–684
10. Papas S, Smith P, Furguson AV (1990) Electrophysiological evidence that systemic angiotensin influences rat area postrema neurons. Am J Physiol 258:R70–R76
11. Jahn K, Bufler J, Weindl A et al (1996) Patch-clamp study on membrane properties and transmitter activated currents of rabbit area postrema neurons. J Comp Physiol 178:771–778
12. Hay M, Lindsley KA (1999) AMPA receptor activation of area postrema neurons. Am J Physiol 276:R586–R590
13. Sorimachi M, Yamagami K, Wakamori M (2002) Expression of P2X receptors on area postrema neurons of rat brain: Studies with fura-2 microfluorometry. Jpn J Physiol 52:suppl. s119
14. Sorimachi M, Yamagami K, Wakamori M (2003) ATP-induced current in area postrema neurons of rat brain: Possible expression of $P2X_2$ receptor. Jpn J Physiol 53: suppl. s203
15. Funahashi M, Mitoh Y, Matsuo R (2002) Nicotinic modulation of area postrema neuronal excitability in rat brain slices. Brain Res 1017:227–233
16. Sorimachi M, Wakamori M (2005) Nicotinic ACh receptor in area postrema neurons of immature rat brain. Neurosci Lett 381:350–353
17. Akasu T, Koketsu K (1985) Effect of adenosine triphosphate on the sensitivity of the nicotinic acetylcholine-receptor in the bullfrog sympathetic ganglion cell. Brit J Pharmacol 84:525–531
18. Nakazawa K, Fujimori K, Takanaka A et al (1990) An ATP-activated conductance in pheochromocytoma cells and its suppression by extracellular calcium. J Physiol (Lond) 428:257–272
19. Searl TJ, Redman RS. Silinsky EM (1998) Mutual occlusion of P2X ATP receptors and nicotinic receptors on symapathetic neurons of the guinea-pig. J Physiol (Lond) 510:783–791
20. Zhou X, Galligan JJ (1998) Non-additive interaction between nicotinic cholinergic and P2X purine receptors in guinea-pig enteric neurons in culture. J Physiol (Lond) 513: 685–697.
21. Barajas-Lopez C, Espinosa-Luna R, Zhu Y (1998) Functional interactions between nicotinic and P2X channels in short-term cultures of guinea-pig submucosal neurons. J Physiol (Lond) 513:671–683
22. Khakh BS, Zhou X, Sydes J et al (2000) State-dependent cross-inhibition between transmitter-gated cation channels. Nature 406:405–410
23. Khakh BS, Fisher JA, Nashmi R et al (2005) An angstrom scale interaction between plasma membrane ATP-gated

$P2X_2$ and $\alpha_4\beta_2$ nicotinic channels measured with fluorescence resonance energy transfer and total internal reflection fluorescence microscopy. J Neurosci 25:6911–6920
24. Boue-Grabot E, Barajas-Lopez C, Chakfe Y et al (1984) Intracellular cross talk and physical interaction between two classes of neurotransmitter-gated channels. J Neurosci 15: 1246–1253
25. Lewis CA (1979) Ion-concentration dependence of the reversal potential and the single channel conductance of ion channels at the neuromuscular junction. J Physiol (Lond) 286: 417–445
26. Grynkiewicz G, Poenie M, Tsien RY (1985) A new generation of Ca^{2+} indicators with greatly improved fluorescence properties. J Biol Chem 260:3440–3450
27. Sorimachi M, Abe Y, Furukawa K et al (1995) Mechanism underlying the ATP-induced increase in the cytosolic Ca^{2+} concentration in chick ciliary ganglion neurons. J Neurochem 64:1169–1174
28. King BF, Ziganshina LE, Pintor J et al (1996) Full sensitivity of P2X2 purinoceptor to ATP revealed by changing extracellular pH. Br J Pharmacol 117:1371–1373
29. Hay M, Hasser EM, Lindsley KA (1996) Area postrema voltage-activated calcium currents. J Neurophysiol 75:133–141
30. Nakazawa K (1994) ATP-activated current and its interaction with acetylcholine-activated current in rat sympathetic neurons. J Neurosci 14:740–750
31. Manalis RS (1977) Voltage-dependent effect of curare at the frog neuromuscular junction. Nature 267:366–368
32. Grassi F, Polenzani L, Mileo AM et al (1993) Blockage of nicotinic acetylcholine receptors by 5-hydroxytryptamine. J Neurosci Res 34:562–570
33. Garcia-Colunga J, Miledi R (1995) Effects of serotonergic agents on neuronal nicotinic acetylcholine receptors. Proc Natl Acad Sci USA 92:2919–2923
34. Sorimachi M, Wakamori M (2004) Inhibitory effect of serotonin on ACh-induced currents in area postrema neurons of rat brain. Jpn J Physiol 54:suppl. s137
35. Fieber LA, Adams DJ (1991) Adenosine triphosphate-evoked currents in cultured neurons dissociated from rat parasympathetic cardiac ganglia. J Physiol (Lond) 434:239–256
36. Rogers M, Dani JA (1995) Comparison of quantitative calcium flux through NMDA, ATP and ACh receptor channels. Biophys J 68:501–506
37. Collo G, North RA, Kawashima E et al (1996) Cloning of P2X5 and P2X6 receptors and the distribution and properties of an extended family of ATP-gated ion channels. J Neurosci 16:2495–2507
38. Kanjhan R, Housley GD, Burton LD et al (1999) Distribution of the P2X2 receptor subunit of the ATP-gated ion channels in the rat central nervous system. J Comp Neurol 407:11–32
39. Atkinson L, Batten TF, Deuchars J (2000) $P2X_2$ receptor immunoreactivity in the dorsal vagal complex and area postrema of the rat. Neuroscience 99:683–696
40. Krishtal OA, Marchenko SM, Obukhov AG (1988) Cationic channels activated by extracellular ATP in rat sensory neutons. Neuroscience 27:995–1000
41. Sorimachi M, Ishibashi H, Moritoyo T et al (2001) Excitatory effect of ATP on acutely dissociated ventromedial hypothalamic neurons of the rat. Neuroscience 105: 393–401
42. Evans RJ, Lewis C, Virginio C et al (1996) Ionic permeability of, and divalent cation effects on, two ATP-gated cation channels (P2X receptors) expressed in mammalian cells. J Physiol (Lond) 497:413–422
43. Virginio C, North RA, Surprenant A (1998) Calcium permeability and block at homomeric and heteromeric P2X2 and P2X3 receptors, and P2X receptors in rat nodose neurones. J Physiol (Lond) 510:27–35